Markos et al. CABI Agriculture and Bioscience (2024) 5:29
https://doi.org/10.1186/s43170-024-00232-3

CABI Agriculture and Bioscience

RESEARCH

Open Access

Modeling performances of maize cultivars under current and future climate scenarios in southern central Ethiopian rift valley

Daniel Markos[1*], Walelign Worku[1] and Girma Mamo[2]

Abstract

Background In southern central rift valley of Ethiopia, maize is an important crop because of its adaptation to wider agro-ecologies and higher yield potential. However, most cultivars were not parameterized to include in the database of Decision Support System for Agro-technology Transfer (DSSAT). As a result simulation of growth and yield of those cultivars was not possible under changing climate.

Methods Two set of independent crop, management and soil data were used for calibration and validation of genetic coefficients of maize cultivars (BH-540, BH-546, BH-547, Shala and Shone) under condition of historic weather (1990–2020). Later, we simulated the growth and yield of maize using twenty multimodel climate ensembles across RCP 4.5 and 8.5 during early, medium and late century across Shamana, Bilate, Hawassa and Dilla clusters using DSSATv4.8 model.

Results Cultivars BH-540, BH-546, BH-547, Shala and Shone produced yields of 5.7, 5.4, 5.2, 6.9 and 7.4 t ha^{-1} with the corresponding error percentage of −0.1, −0.8, −1.0, −6.1 and 2.6%. The results of normalized root mean square were 1.14–4.2 and 3.0–3.9%, for grain yield during calibration and validation, respectively showing an excellent rating. The simulation experiment produced 5.4–9.2 t ha^{-1} for grain yield of maize cultivars across the study areas, which is likely to fall close to 63.3% by 2070 if right adaptation options are not introduced necessitating switch in cultivars and production areas.

Conclusions There is critical need for reduction of GHGs emissions, generation of innovative adaptation strategies, and development of drought and heat stress tolerant maize cultivars. Hence, researchers and policy makers shall act with utmost urgency to embark with breeding programs that target climate change adaptation traits in maize crop.

Keywords Calibration, DSSAT model, Maize, Simulation, Validation

*Correspondence:
Daniel Markos
studentdaniel77@gmail.com
[1] School of Plant and Horticultural Sciences, Hawassa University, P.O.Box-05, Hawassa, Ethiopia
[2] Ethiopian Institute of Agricultural Research, P.O.Box-2003, Addis Ababa, Ethiopia

Introduction

Assessment of crop yield response to climate risks is commonly carried out using either machine learning, regression, or process-based tools (Leng and Hall 2020). Since recently, process-based models are being used to simulate crop growth and development by integrating genotypic, environmental, and management information (Kalra et al. 2008) into a comprehensive expression. The same is used to evaluate the impact of climate on crop production as a result of increased greenhouse gases emission into the atmosphere (White et al. 2011), and to generate compatible adaptation responses for sustainable agricultural production (Aggarwal et al. 2006). One of the contemporary support tools is DSSAT; in which a set of independent modules that operate simultaneously using soil, climate, crop, and agronomic management databases (Jones et al. 2003). In Ethiopia, improved decision support tools (DSTs) have been in use over the last couple of decades in the interest of modernizing research data for improving agricultural productivity under varying climate scenarios (Yimer et al. 2022; Feleke et al. 2021; Liben et al. 2018; Jemal 2018; Kassie et al. 2014). However, the progress in using crop models in agronomic studies and accurate simulation of crop production for different agro-ecological conditions has been slow due to the complexity of the relevant biophysical processes associated with uncertainty (Feleke et al. 2021), and the scarcity of relevant datasets (Leng and Hall 2020).

It is crucial to expand the body of information about site-specific calibration and validation procedures, particularly the identification of crop cultivar-specific genetic coefficients for crop model evaluation, in order to logically guide the application of crop-climate modeling research (Hoogenboom et al. 2010). With the use of these genetic factors, crop models can more accurately simulate how different genotypes perform in a range of soil, weather, and management scenarios. Because it requires costly and time-consuming field trials, estimating the genetic coefficients is the most complex part of crop-climate modeling (Lamsal et al. 2018). Because of this, determining the genotype specific parameters (GSPs) before using the cropping system model is challenging. For various Ethiopian maize cultivars, there have been efforts that have produced cultivar coefficients (Mohammed et al. 2021, Liben et al. 2018; Kassie et al. 2014). For some maize cultivars cultivated specifically in the southern central rift valley, cultivar criteria were not established, though. Therefore, there is a compelling argument to calibrate the DSSAT maize model using cultivar coefficients and to periodically update or parameterize crop modeling dataset with new cultivars (Holzworth et al. 2015).

It is feasible to estimate multi-year and multi-location data from breeder assessment studies across different agro-climatic conditions by using the GSPs, which offer the genotype component of G×E×M interactions (Lamsal et al. 2018; Jones et al. 2003). In actuality, depending on the process and the crop model, the cultivar coefficients hold genetic, phenological, and physiological information of a specific crop variety, enabling simulations at the daily or, in some situations, hourly time steps. The crop's vegetative and reproductive development stages are also reorganized, and the plant and soil water, nitrogen, phosphorus, and carbon balances are updated daily as the growing season progresses (Hoogenboom et al. 2010). The DSSAT model then models growth and development in relation to GSPs, weather, soil, and crop management decisions. According to Jones et al. (2013), the genetic inputs are P1 (thermal time from seedling emergence to the end of the juvenile phase), P2 (measures development about photoperiod), P5 (measures the thermal time from silking to physiological maturity), and PHINT (thermal time between the appearance of leaf tips).

Because of susceptibility of current production systems to climate change, there are serious risks to the sustainability of maize production in the tropics. The performance of maize varieties in China (Zhang et al. 2021; Li et al. 2022), Nigeria (Tofa et al. 2021), and the East African area (Araya et al. 2015; Ojara et al. 2021) was predicted by a number of writers. According to their reports, China's maize cultivation areas would decrease by 53% under the RCP 4.5 and RCP 8.5 emission scenarios in 1950s (Zhang et al. 2021); in northern Nigeria, the reduction would be as high as 43% by the end of century (Tofa et al. 2021), and in East Africa region would be as high as 40–60% during the mid century (Ojara et al. 2021). Shorter growing seasons, pest and disease outbreaks, flooding and crop failures (Luhunga et al. 2018; Niang et al. 2014), rising air temperatures (Luhunga et al. 2018), heat and water stresses (Pereira 2017), rising evaporative demand (Ongoma et al. 2018), and declining water availability (Shivakumar et al. 2019) were the factors expected to cause a decline in yield. These factors ultimately limit land suitability and productivity (Whisler et al. 1986). However, there is no assessment of how different kinds of maize varieties would react to a changing climate under RCP 4.5 and 8.5 in the early, mid- and late centuries in the southern central rift valley of Ethiopia.

Prior to release, the maize CERES module in the DSSAT provides an opportunity to investigate the potential of any new cultivars and crop management techniques in various environments (soil, climate, and management) by analyzing growth duration, growth rate, and the degree to which stresses affect these processes (Ritchie and Nesmith 1991). Because the input files are cultivar-specific, a user may model crop growth, development, and yield for several varieties of maize with few modifications (Boote et al. 2010, 2017).

Keeping these imperatives in view, the present study was undertaken to determine the genetic coefficients of maize cultivars adapted to the southern central rift valley of Ethiopia and to simulate the growth and yield of maize across various environments under present and future climate conditions.

Materials and methods

Description of the study area

This study was carried out in southern plains of central rift valley of Ethiopia, located between 6° 22′ 48" N to 7° 43′ 12″ N latitudes. The Western margin corresponds to 37° 45′ 0″ E to 38° 40′ 48″ E longitudes, covering an area of 1,021,332 ha (Fig. 1). The study area has been divided into four distinct clusters (Shamana, Bilate, Hawassa and Dilla areas) (Markos et al. 2022).

DSSAT CERES-Maize module

The International Benchmark Sites Network for Agrotechnology Transfer Project (IBSNAT, 1994) brought together a global network of scientists to produce DSSAT. Multiple previous versions of the DSSAT mimic crop growth, development, and yield by utilizing minimal meteorological data, crop management data, and soil profile characteristics that have been preset. According to Jones et al. (2013), crop cultivar, planting date, row and plant spacing, fertilizer-N levels, tillage techniques, and organic amendments are some of the crop management parameters needed to calibrate the DSSAT model. Additionally, phenological stage inputs like blooming dates and days to maturity are included in the data. Maximum and lowest temperatures (°C), solar radiation (hr), and rainfall (mm) are the minimal meteorological data sets that are needed. Depth and the physical and chemical characteristics of the soil make up the parameters of the soil profile (Wang et al. 2021) on crop management were kept track of during the growing seasons. For the purpose of calibrating and validating the CERES-Maize module, input files such as weather, soil, experimental, and A & T (average measured data file, annual as well as temporal) were produced. For calibration, the CERES-Maize module needs a set of six cultivar-specific characteristics (Table 3). Whilst the four (P1, P2, P5, and PHINT) regulate the timing of phenological phases, G2 and G3 describe the potential yield under ideal circumstances (Hai-long et al. 2017).

Determination of crop genetic coefficients

Genetic coefficients particular to each cultivar are needed for the DSSAT crop model calibration in order to accurately depict the processes associated with growth and development under varying weather, soil, and management circumstances. Observed days to flowering, days to physiological maturity, and grain yield of maize cultivars, that were under field experiments between 2013 and 2017, were used to estimate genetic coefficients (Deribew and Dawuro, 2012; Mekasha et al. 2013; Shegenu and Tilahun 2015; Sorsa and Mesfin 2015). The genetic coefficients for the cultivars of maize BH-540 and

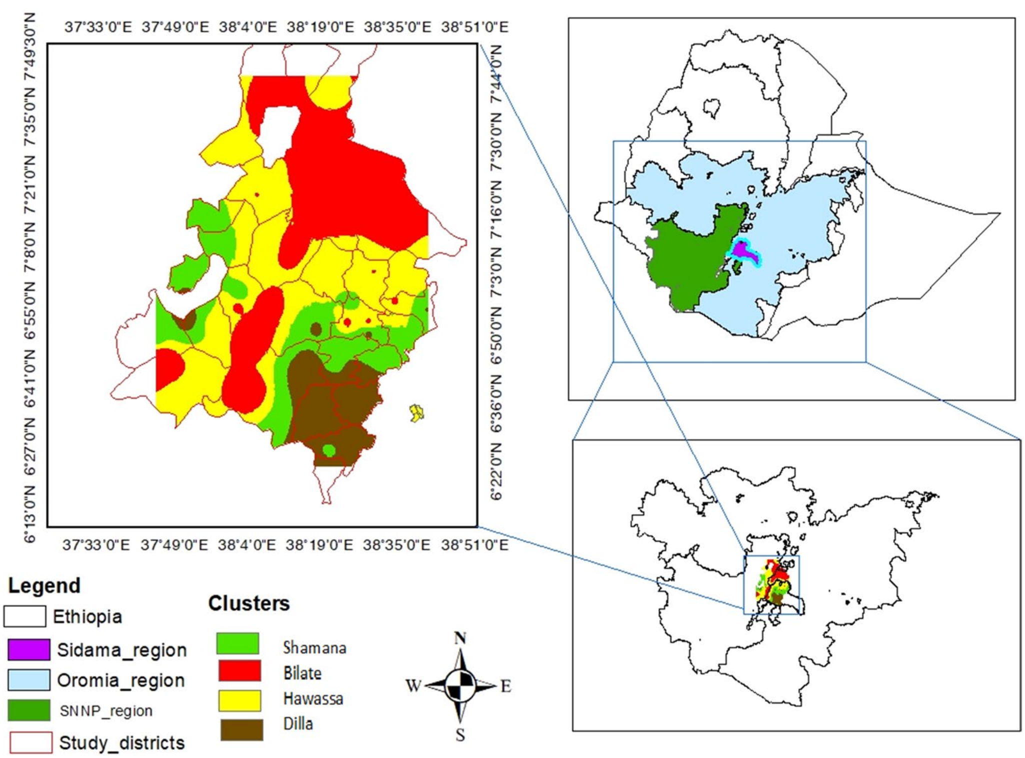

Fig. 1 The study area map with the four distinct clusters

BH-546, as indicated in Table 3, were adopted from Liben et al. (2018), Kassie et al. (2014), and Mohammed et al. (2021). However, BH-547, *Shala* (P2859W), and *Shone* (PHB30G19) cultivars do not have genetic coefficients in DSSAT that have been included before. The medium maturity cultivar group BH-546, which is already accessible in the DSSAT for modification and use for BH-547, provided the initial values of the genetic coefficients. Since the cultivars *Shala* and *Shone* are pioneer hybrids, the medium maturing pioneer file (such as PIO-3183) was chosen from the DSSAT database and applied to the new cultivars by making modifications to it. To conduct the simulation, the computed crop specific parameters (CSPs) for the cultivars BH-547, *Shala*, and *Shone* were transferred into the MZCER048 CUL file. Through trial and error modifications, an iterative technique was utilized to acquire an appropriate genetic coefficient until the dates of anthesis, physiological maturity, and grain production were matched between the simulated and observed values (Ma et al. 2006). The obtained genetic coefficients were eventually applied to assess the effectiveness of the model.

Historic weather

Historic weather data of the growing season during the last thirty years (1991–2020), including daily precipitation (mm), minimum and maximum air temperatures (°C), and sunshine hours were collected from different sources; including the Ethiopian Meteorological Institute (EMI), Hawassa Branch office and Hawassa Agricultural Research Center (HARC). In the absence of meteorological stations data, Climate Hazards Group Infra-Red Precipitation with Stations (CHIRPS) satellite rainfall data (https://data.chc.ucsb.edu/products/CHIRPS-2.0/) were used (Dinku et al. 2018; Belay et al. 2021; Bayable et al. 2021). The CHIRPS data were shown to be identical to ground rainfall ($p > 0.05$) based on the t test, with the exception of a few stations (Mulungu and Mukama 2023). Solar radiation (MJ m^{-2} d^{-2}) was derived from daily sunshine hours by using WEATHERMAN of DSSAT. The weather files were created by using WEATHERMAN module of DSSAT for running of the model.

Climate scenarios

The baseline daily climate data (1980–2010) were used to simulate the future climate across 20 GCMs (Global circulation models) with RCP (Representative concentration pathway) 4.5 and RCP 8.5. XLSTAT was used to prepare the climate scenarios in the form required by DSSAT crop model (Rani et al. 2023). Future climate change data of contrasting multi-model ensembles of 20 Global Climate Models (GCMs) were accessed using Coordinated Regional Climate Downscaling Experiment (CORDEX) (Giorgi et al. 2009) which were downscaled to 44 km horizontal resolution (https://esgf-node.llnl.gov/search/esgf-llnl/). Sponsored by the World Climate Research Program, CORDEX generated high-resolution future climate projections by downscaling GCM using different regional climate models (Table 1). A 30-year window period representing climate projections by the near term/early century (2011–2039), mid-term/midcentury (2040–2069) and end-term/late century (2070–2100) was considered. First, moderate pathway emission scenario (RCP 4.5) was selected, as the radiative forcing does not diverge in the different RCPs by the selected time horizon (Riahi et al. 2008; Moss et al. 2010; Willems and Vrac 2011).

RCP 4.5 represents the moderate emission scenarios. It is a stabilization scenario where total radiative forcing is stabilized around 2050 by employment of advanced technologies for reducing greenhouse gas emissions (Clarke et al. 2007). Next, the highest emission (RCP 8.5) or strong forcing scenario with 8.5 W/m2 is the extreme (warmest), under high population and advanced technology was selected for each RCP, which is characterized by increasing greenhouse gas emissions and concentration in the atmosphere.

Table 1 The multimodal climate ensembles used to downscale climate data for East Africa

GCM/RCM	CCLM 4.8	CNRM -CM5	HIRHAM 5	RACMO 22 T	RCA 4	REMO	Reg CM4	SOMD -ESD	RCP 4.5	RCP 8.5
CNRM-CM5	√				√			√	√	√
GFDL-ESM2M					√			√	√	√
ICHEC-EC-EARTH	√		√	√	√	√			√	√
MIROC5					√			√	√	√
MIROC5-ESM								√	√	√
MIROC5-ESM-CHEM								√	√	√
MPI-ESM-LR r1	√	√			√	√			√	
MPI-ESM-LR r1	√				√	√	√			√
NORESM1-M			√		√				√	√

Source: http://www.csag.uct.ac.za/cordex-africa

Soil characterization

The summary of the soil data collected and stored in the soil input file (Table 2). The soil texture, bulk density, soil moisture, pH, organic matter, total N, field capacity, wilting point, and saturated moisture content were captured for each cluster (Table 2). The top soils of the experimental sites were specified as silty clay, sandy clay loam, loam and clay in *Shamana*, *Bilate*, *Hawassa* and *Dilla* clusters, respectively.

Table 2 Physical properties of the experimental soils

Depth (cm)	SAT UL	FC DUL	PWP LL	Bulk density (g/cm^{-3})	Texture		
					%Clay	% silt	% sand
Bilate							
0–38	0.39	0.34	0.25	1.25	20	28	52
38–78	0.39	0.32	0.26	1.36	20	24	56
78–102	0.40	0.32	0.26	1.37	20	24	56
102–171	0.40	0.31	0.27	1.26	22	22	56
171 +	0.40	0.29	0.28	1.43	20	14	66
Dilla							
0–38	0.41	0.28	0.13	1.2	51	21	28
38–78	0.38	0.25	0.15	1.32	29	41	30
78–102	0.38	0.26	0.19	1.34	47	33	20
102–171	0.39	0.27	0.20	1.42	35	29	36
Hawassa							
0–25	0.52	0.26	0.11	1.36	22	38	40
26–69	0.52	0.24	0.09	1.36	24	36	40
70–115	0.43	0.22	0.07	1.55	26	30	44
116–131	0.40	0.20	0.05	1.57	32	34	34
132–157	0.36	0.18	0.03	1.63	10	40	50
158–187	0.31	0.16	0.02	1.58	10	54	36
Shamana							
0–15	0.54	0.42	0.19	1.29	51	43	6
15–30	0.57	0.40	0.17	1.34	39	53	6
30–60	0.59	0.39	0.17	1.33	35	59	6
60–90	0.53	0.33	0.15	1.33	41	53	6

Source: Demis and Beyene (2010), Wondimeneh (2010), Ayalew et al. (2015) and Jemal (2015)

SAT UL: saturation point upper limit; FC DUL: field capacity drained upper limit; PWP LL: permanent wilting point lower limit

Table 3 Genetic coefficients of maize cultivars

Coefficient	Definition	Maize cultivars				
		BH 540	BH 546	BH 547	*Shala*	*Shone*
P1	The span of time (measured in ˚C days, above a base temperature of 8˚C) between the emergence of seedlings and the conclusion of the juvenile phase, during which the plant is not susceptible to variations in photoperiod	245	253	260	250	320
P2	The amount that development (measured in days) is postponed for every hour that the photoperiod is extended over the longest photoperiod (which is thought to be 12.5 h)	0.60	0.7	0.8	1.42	0.52
P5	Thermal period (measured in ˚C days above a base temperature of 8 ˚C) from silking to physiological maturity	850	945	950	942	962
G2	Maximum possible number of kernels per plant	780	490	440	484	470
G3	Kernel filling rate during the linear grain filling stage under optimum conditions (mg day^{-1})	8.5	12.7	14.8	14.6	10.0
PHINT	Phyllochron interval, the interval in thermal time between successive leaf tip appearances (˚C day)	48	49	54.4	48.4	74.91

DSSAT crop model calibration

The genetic coefficients were used for model calibration together with, historic weather data, crop management and soil properties during 2014–2015 cropping season. Comparisons between observed and simulated maize yield and its attributes were evaluated using RMSE, d-statistic and R^2 as shown in Eqs. 1, 2 and 3 (Abera et al. 2018).

$$\mathrm{RMSE}\,(\mathrm{kgha}^{-1}) = \frac{\sqrt{\sum(\mathrm{Yi}-\mathrm{Xi})^2}}{\mathrm{n}} \tag{1}$$

where Xi and Yi are the observed and simulated values respectively and n is the number of observations. Small values of RMSE considered as indicators for good performance of the DSSAT model. The RMSE values closer to zero imply a good fit between observed and simulated yields. A zero RMSE values mean that the model predicts the observations with perfect accuracy. The RMSE values closer to 0 indicate better agreement between the simulated and observed values. The second criterion i.e. the normalized RMSE (nRMSE) is expressed as the ratio between the RMSE and the average of the observed data.

$$\mathrm{nRMSE} = \frac{\mathrm{RMSE} * 100}{O^{-}} \tag{2}$$

where O^{-} stands for the overall mean of observed values. The model simulations were considered excellent, good, fair, and poor, respectively, based on the nRMSE values of < 10%, 10–20%, 20–30%, and > 30%. The third criterion was the determination of index of agreement or d-statistic (Willmott, 1982). It is used to measure the degree of the model prediction error, and the following Eq. 3 was used:

$$\mathrm{d} = 1 - \frac{\sum(\mathrm{Yi}-\mathrm{Xi})^2}{\sum(!\mathrm{Yi}-\mathrm{Xm}!+!\mathrm{Xi}+\mathrm{Ym}!)^2} \tag{3}$$

where Yi, and Ym are simulated and mean of the simulated yield, respectively. Similarly, Xi and Xm are the observed and mean of observed yields, and n is the number of observations. The d values range between 0 (no agreement) and 1 (perfect fit). d values closer to 1 are considered as good performance of the DSSAT model (Yang et al. 2014). The correlation coefficient (r) value, which is used to assess the strength of the association between the simulated and observed values in units ranging from −1 to 1, was the third criteria (Gupta et al., 1999). This is done in order to confirm the dependability of the model by statistical analysis, which includes correlation determination (R2). Consequently, r evaluates the linear model's "goodness of fit," with r = 1 denoting a perfect match and r = 0 denoting the absence of a linear relationship as shown in Eq. 4.

$$\mathrm{R}^2 = \frac{\mathrm{n}(\sum \mathrm{xy}) - (\sum(\mathrm{x})\sum(\mathrm{y}))}{\sqrt{(n\sum x^2 - (\sum_x)^2)(n\sum_y 2 - (\sum_{y)}\, 2)}} \tag{4}$$

where n is the number of model and observation data points, x is the model data, and y is the observation data.

Model validation

Model performance was evaluated by comparing the simulated versus observed values from the independent experimental data of 2016–2018 as reported by numerous authors (Bejigo 2018; Loha and Hidoto 2018; Hidoto 2021; Hidoto and Markos 2019). The comparison of observed and simulated data on anthesis date, physiological maturity date and grain yield was carried out by analyzing the results from Eqs. 1, 2 and 3, mentioned above. These authors considered cultivars BH-540, BH-546, BH-547, *Shala* and *Shone* among others. All these cultivars are medium maturity category, with varying yield potential and adaptability, but grown in areas with rainfall range of 450 to 750 mm.

Simulation experiment

Performance of five maize cultivars (BH-540, BH-546, BH-547, *Shala* and *Shone*) commonly grown across four locations (*Shamana*, *Bilate*, *Hawassa* and *Dilla*) was simulated using the cultivar parameters of each genotype, edaphic conditions and historic weather for each location. For this experiment, recommended dates of planting (18th January for *Shamana*, May 1st for Bilate, April 20th for *Hawassa* and March 20th for *Dilla*), nitrogen application (92 kg ha^{-1} N for *Shamana*, 46 kg ha^{-1} N for *Bilate*, 92 kg ha^{-1} N for *Hawassa* and 69 kg ha^{-1} N for *Dilla*), and conventional tillage method and population (53,333 plants ha^{-1}) were employed. The second analysis considered climate data from contrasting multi-model ensembles of 20 Global Climate Models (GCMs) and accessed by using Coordinated Regional Climate Downscaling Experiment (CORDEX) across RCP 4.5 and 8.5. The crop management inputs were similar in both experiments. Both simulation experiments were run under water and nitrogen limiting conditions representing current management scenario for rain-fed farming conditions during early, mid- and late century using a thirty year period as replications (Feleke et al. 2021).

Statistical analyses for simulation experiment

The outputs of DSSAT model for dates of anthesis and maturity, and grain yield at harvest were statistically analyzed using the analysis of variance (ANOVA) technique to evaluate the impact of climate change on maize production. Prior to ANOVA, homogeneity of variance across clusters was assessed using Levene (1960), O'Brien (1981), and Brown and Forsythe tests (1974).

Accordingly, the five cultivars were evaluated across four locations for each GHGs emission scenario during baseline, early, mid- and late century. The year effect, which has 30 levels, was used as replications (blocks) in the DSSAT software because the maize yield in 1 year under a given treatment was not affected by another year. Since each simulation year had unpredictable weather conditions, formal randomization of simulation years was not needed (Chambers et al. 2017). The ANOVA was calculated using the SAS software package and treatments averages were separated using least significance difference (LSD) at 5% level of probability wherever difference between averages existed.

Cumulative distribution function (CDF)

This research also involved the analyses of an array in risks associated with growing the test maize cultivars under four geographic clusters. For the risk analyses, we employed the technique of non-exceedance probability (P). The non-exceedance technique is the probability that a yield value would be less than a user defined value during certain time series and under a given technological level (Gobo and Abam 2006). For thirty-year time series data arranged in descending order with rank r, return period (T) = 1/r, then the non-exceedance probability (CDF) was approximated by a plotting position formula (Eq. 5)

$$\mathrm{F}i = \frac{ri - b}{n + 1 - 2b} \tag{5}$$

where F is the probability associated with observation i, r is the rank number of the observation from highest to lowest, n is the number of observations and b is the slope between observations and years of occurrence. The slope enabled to weigh the contribution of each event to the computation of the non-exceedance probability. In conjunction with risk analyses, we have also conducted the targeted yield analyses, of which the resulting information helps in categorizing the farmers according to their attitude toward risk.

Estimation of yield changes under different climate scenarios

The biophysical impact of climate change across southern central rift valley was obtained by calculating changes in crop yield between the current and the proposed adaptation responses for maize cultivars. Then the changes were calculated for each of the early, mid and late century periods, relative to the current practice for the respective GHGs emission scenarios. Accordingly, impacts of adaptation responses were computed based on Feleke et al. (2021) as given in Eq. 6.

$$\text{Yield change}(\%) = \frac{\left(Yf - Yb\right) * 100}{Yb} \tag{6}$$

where Yf—simulated yield of a cultivar under new emission scenarios; Yb—simulated yield of a cultivar under baseline scenario.

Results

Model calibrations for southern central rift valley of Ethiopia

Table 3 displayed the crop genetic coefficients that were obtained. The cultivars of BH-540, BH-546, BH-547, *Shala*, and *Shone* have P1 values of 245, 253, 260, 250, and 320 ˚C, respectively. In actuality, this indicates that the *Shone* maize variety arrived at the essential growth phases later than other cultivars since it needed more thermal time from the time the seedlings emerged to the conclusion of the juvenile phase. For the same cultivars, the P2 was 0.60, 0.7, 0.8, 1.42, and 0.52 days in that respective order. Comparably, for BH-540, BH-546, BH-547, *Shala*, and *Shone*, the corresponding P5 values were 850, 945, 950, 942, and 962 ˚C day; G2 was 780, 490, 440, 484, and 470; and PHINT was 48, 49, 54.4, 48.4, and 74.1 in that same order. Thus PHINT that determines the length of vegetative growth in maize, which is longer in temperate climates but shorter in tropical ones is almost similar for all cultivar except *Shone* (Table 3).

Days to anthesis for BH-540, BH-546, BH-547, *Shala*, and *Shone* were 87, 82, 83, 78, and 82 during calibrations, with corresponding error percentages of 5.7, 8.5, 13.3, 7.7, and 4.9% (Table 4). The mean number of days to maturity for each study location was 136, 138, 155, 144, and 154, with corresponding error percentages of 2.2, 2.9, 5.2, 6.9, and 2.6 in that respective order. For BH-540, BH-546, BH-547, *Shala*, and *Shone*, the correspondingly obtained grain yields were 5.7, 5.4, 5.2, 6.9, and 7.4 t ha-1 with error percentages of −0.1, −0.8, −1.0, −6.1, and 2.6.

Model validation for southern central rift valley of Ethiopia

Days to anthesis during validation research were 81, 75, 72, 72, and 78 for BH-540, BH-546, BH-547, *Shala*, and *Shone*, with corresponding error percentages of 1.2, 7.4, 11.1, 7.7, and 4.9% (Table 4). With error percentages of 7.0, 6.0, −2.8, 5.6, and −4.2, respectively, the average days of maturity across research locations were 143, 134, 143, 142, and 144. With error percentages of −6.0, −8.8, −2.9, −11.0, and 2.6 for BH-540, BH-546, BH-547, *Shala*, and *Shone*, respectively, the final grain yields that were obtained were 5.6, 5.3, 5.9, 7.5, and 7.4 t ha^{-1}. The error % was therefore greatest for days to anthesis, middle for days to maturity, and lowest for grain yield parameter. Days to anthesis for BH-540, BH-546, BH-547, *Shala* and *Shone* cultivars

Table 4 Observed and simulated values for days to anthesis, days to maturity and grain yield at harvest during model calibration using historic weather

Traits	BH-540	BH-546	BH-547	*Shala*	*Shone*
HWAMS					
Observed (t ha^{-1})	5.7	5.4	5.2	7.3	7.2
Simulated (t ha^{-1})	5.7	5.4	5.2	6.9	7.4
Error %	−0.1	−0.8	−1.0	−6.1	2.6
R^2	1	0.98	1	1	1
RMSE (t ha^{-1})	0.07	0.24	0.24	0.26	0.24
nRMSE (%)	1.14	3.90	3.90	4.22	3.90
d-Stat	1	0.98	0.79	0.84	0.69
ADATS					
Observed (days)	82	75	72	72	78
Simulated (days)	87	82	83	78	82
Error %	5.7	8.5	13.3	7.7	4.9
R^2	0.94	0.92	0.87	0.96	0.86
RMSE (days)	7.07	6.52	6.5	6.49	7.07
nRMSE (%)	9.3	8.6	8.6	8.6	9.3
d-Stat	0.9	0.75	0.8	0.82	0.81
MDATS					
Observed (days)	133	134	147	134	150
Simulated (days)	136	138	155	144	154
Error %	2.2	2.9	5.2	6.9	2.6
R^2	0.89	0.87	0.98	0.87	1
RMSE (days)	7.07	9.7	7.03	2.56	9.31
nRMSE (%)	5.1	6.9	5.0	1.8	6.7
d-Stat	0.78	0.65	0.92	0.74	0.81

ADAT—days to anthesis; MDAT—days to maturity; HWAMS—grain yield

Table 5 Observed and simulated values for days to anthesis, days to maturity and grain yield at harvest during model validation using historic weather

Traits	BH-540	BH-546	BH-547	*Shala*	*Shone*
HWAMS					
Observed (t ha^{-1})	5.9	5.8	6.0	8.3	7.2
Simulated (t ha^{-1})	5.6	5.3	5.9	7.5	7.4
Error %	−6.0	−8.8	−2.9	−11.0	2.6
R^2	0.88	0.93	1	0.97	0.94
RMSE (t ha^{-1})	0.20	0.24	0.24	0.26	0.24
nRMSE (%)	3.0	3.6	3.6	3.9	3.6
d-Stat	0.82	0.99	0.495	0.64	0.89
ADATS					
Observed (days)	81	75	72	72	78
Simulated (days)	82	81	81	78	82
Error %	1.2	7.4	11.1	7.7	4.9
R^2	0.82	0.92	0.90	0.95	0.95
RMSE (days)	2.19	6.52	2.5	6.49	11.1
nRMSE (%)	2.9	8.6	3.3	8.6	14.7
d-Stat	0.71	0.85	0.64	0.72	0.81
MDATS					
Observed (days)	133	126	147	134	150
Simulated (days)	143	134	143	142	144
Error %	7.0	6.0	−2.8	5.6	−4.2
R^2	0.89	0.94	0.88	0.92	0.96
RMSE (days)	7.35	9.79	7.03	9,28	9.31
nRMSE (%)	5.4	7.2	5.2	6.7	6.8
d-Stat	0.88	0.75	0.72	0.82	0.93

ADAT—days to anthesis, MDAT—days to maturity and HWAMS—grain yield

were 82, 81, 82, 78, and 81 according to the validation results, with corresponding goodness of fit (R^2) values of 0.82, 0.92, 0.90, 0.95, and 0.95 between observed and simulated estimations (Table 5). For cultivars BH-540, BH-546, BH-547, *Shala*, and *Shone*, respectively, had the goodness of fit (R^2) between the observed and simulated anthesis date was 0.96, 0.94, 0.88, 0.92, and 0.89, displaying error percentages of 7.0, 6.0, −2.8, 5.6, and −4.2 (Table 5).

During the validation experiment, the RMSE results for grain yield, anthesis dates, and maturity dates were 0.2–0.26 t ha^{-1}, 2–11 days, and 7 to 9 days, respectively. These values equate to 3.0–3.9, 2.9–14.7, and 5.2–7.2%, respectively, for normalized root mean square percentage; great ratings for grain yield and maturity dates, but good ratings for anthesis dates, are indicated by these values. For the cultivars *Shone*, *Shala*, and BH-546, on the other hand, grain yield values were below the 1:1 line, indicating that the model underestimated grain yield (Fig. 2a). Grain yield's regression line was roughly in line with the 1:1 line, suggesting a better agreement.

For cultivars BH-540, BH-546, BH-547, *Shala*, and *Shone*, the d-statistic values were 0.77, 0.72, 0.95, 0.95, and 0.76% in the event that there was a trend run between the observed and simulated values. Thus, better modeling agreement was shown by the d-statistic values.

Mean separation of days to flowering, days to maturity, and yield

Because variances of the data are equal (homogenous) across different locations, combined analysis was performed for all locations. Results showed that variety *Shala* (7.6 t ha^{-1}) produced significantly ($P<0.05$) higher yield, compared to cultivars BH-540, BH-546 and BH-547 in *Shamana* cluster (Table 6). However, there was no statistical yield difference between yield values of variety *Shala* (7.6 t ha^{-1}) and *Shone* (7.0 t ha^{-1}). In *Shamana*, BH-547 produced statistically lower maize yields (2.2 t ha^{-1}). In *Bilate* cluster, cultivar *Shone* produced significantly higher yield (5.4 t ha^{-1}) compared to other cultivars. In *Hawassa* cluster, cultivar *Shone* was statistically superior (9.2 t ha^{-1}) to the other cultivars. The lowest

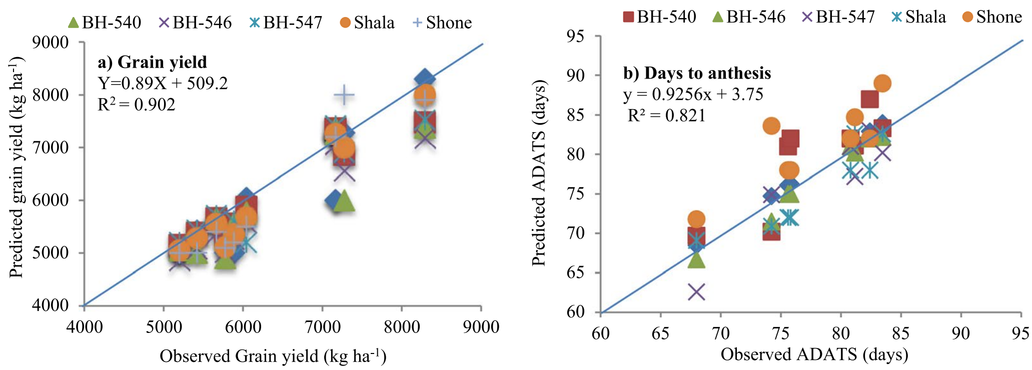

Fig. 2 Relationship between simulated and observed **a** grain yield **b** days to anthesis

Table 6 Means of simulated harvest yield (t ha^{-1}) at maturity and anthesis dates using historic weather

Variety	Clusters			
	Shamana	Bilate	Hawassa	Dilla
HWAMS* (t ha^{-1})				
BH-540	3.9e**	3.9e	7.6bc	3.6e
BH-546	3.6ef	3.9e	7.1c	4.1e
BH-547	2.2g	4.3e	8.2b	3.4f
Shala	7.6bc	4.1e	7.6b	4.1e
Shone	7.0c	5.4d	9.2a	5.9d
LSD0.05	0.77*			
CV (%)	18.01			
ADATS (days)				
BH-540	81.1fg	69.7jk	83.3f	70.2ij
BH-546	80.2g	66.7l	82.2g	71.5kl
BH-547	77.2e	62.6i	80.2d	74.90h
Shala	82.6f	69.1k	82.6f	70.9ijk
Shone	84.7b	71.8de	89.0a	83.6c
LSD0.05	2.13*			
CV (%)	2.81			

*ADATS, MDATS and HWAMS represent simulated days to anthesis, days to maturity and grain yield

**Values followed by different letters show presence of significant difference at 0.05% level of probability

yield in *Shamana* cluster was measured due to BH-546 (7.1 t ha^{-1}). In *Dilla* cluster, cultivar *Shone* produced 5.9 t ha^{-1}, which is significantly higher than the other cultivars tested in this experiment.

Cumulative frequency distribution (CFD) of grain yield across clusters

Figure 3 below summarizes the risks of production for maize cultivars across the geographic clusters in Southern Region of Ethiopia; Fig. 3A shows that *BH-540* is least productive under Dilla climate, where the risk of getting two tons ha^{-1} is 25%, while 6.8 t ha^{-1} of *BH-540* is produced at the same risk level under Hawassa climate. Despite there was a cross over between Shamana and Bilate at the middle of the two curves, the remaining 50% of the data distribution showed a better performance for Shamana compared to Bilate. Under Shamana climate, achieving 5.8 t ha^{-1} of *BH-540* is possible; but the associated risk is 75%. Further, achieving 4.1 t ha^{-1} of *BH-540* under Shamana climate is possible, but the risk would be 50% while 7.5 t ha^{-1} of the same cultivar is achieved under Hawassa climate at 50% risk. At 75% risk level, 2.2 t ha^{-1} of *BH-540* is produced under Dilla climate, 4.8 t ha^{-1} at Bilate, 5.8 t ha^{-1} at Shamana and 9 t ha^{-1} under Hawassa climate. Overall, *BH-540* is not recommended to be grown under Dilla climate, while Hawassa is the best for this cultivar.

Figure 3B shows that, cultivar *Shone* yields about 2 t ha^{-1} under Dilla climate at 50% risk level. Under the same risk, *Shone* produces 5.8 t ha^{-1} at Bilate, 7.8 t ha^{-1} at Shamana and 9.8 t ha^{-1} at Hawassa. At 75% risk level, 2.2 t ha^{-1} of *Shone* is produced under Dilla climate, 6 t ha^{-1} at Bilate, 8.1 t ha^{-1} at Shamana and 10 t ha^{-1} under Hawassa climate. As can be noted from Fig. 3B, a risk averse farmer, targeting lower yields in Dilla cluster, would plant cultivar *Shone* with the correspondingly low risk; that is why the risk level to get 2 t ha^{-1} is also less than 25%. Figure 3C describes the productivity of cultivar *Shala* across the maize production clusters in the study area. *Shala* demonstrated results approximating the pattern of BH-540, except differences in absolute values. As can be noted, at 75% risk level, 2.4 t ha^{-1} of *Shala* is produced under Dilla climate, 5 t ha^{-1} at Bilate, 5.5 t ha^{-1} at Shamana and 8.8 t ha^{-1} under Hawassa climate. At 50% risk level, *Shala* yields 2.2 t ha^{-1}at Dilla, 4 t ha^{-1} at Bilate and Shamana, and 7.8 t ha^{-1} at Hawassa conditions. Although there are some inconsistencies, the responses of BH-540, BH-546 and *Shala* had similar pattern.

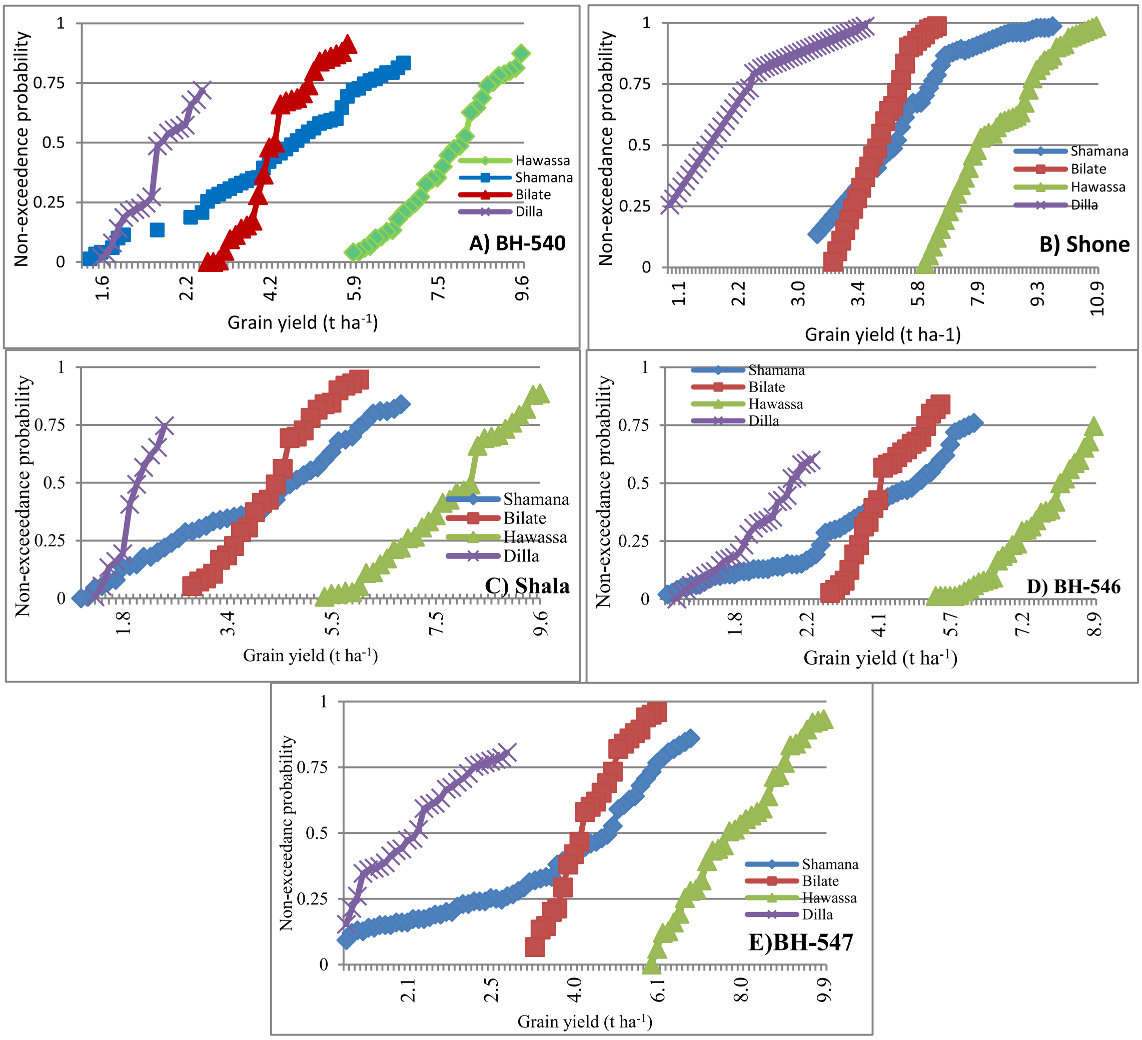

Fig. 3 Risk/probability of non-exceedance of harvested yield of maize varieties across the clusters

At 50% risk (Fig. 3D) *BH-546* yields 2.2 t ha^{-1} at Dilla, 3.6 t ha^{-1} at Bilate and Shamana, and 7.2 t ha^{-1} at Hawassa conditions. At 75% risk, the achievable productivity of BH-546 is 2.4 t ha^{-1} under Dilla climate, 4.4 t ha^{-1} for Bilate, 5 t ha^{-1} for Shamana and 7.8 t ha^{-1} for Hawassa climate. For BH-547 (Fig. 3E*)*, the cross over between Shamana and Bilate shows cultivar BH-547 is more productive at Bilate than Shamana at the lower technological levels, but using more advanced technology turns high productivity i.e. for the upper side of the data distribution for the same cultivar. With the 75% risk, productivity is 2.5 t ha^{-1} for Dilla, 5 t ha^{-1} for Bilate, 6 t ha^{-1} for Shamana and 9 t ha^{-1} for Hawassa. At 50% risk level, *BH-547* yields 2.2 t ha^{-1} at Dilla, 4.5 t ha^{-1} at Bilate and Shamana, and 8 t ha^{-1} at Hawassa conditions. Such risk analyses help to categorize farmers into risk averse, risk neutral and risk takers. Obviously, the more the risk averse behavior, the more the downside production risk and therefore, such famers remain reluctant to adopt improved technologies. Farmers aiming at higher yield (upside production risk takers) are more ready to adopt those technologies responsive to the production risk prevailing under a given climate. By disaggregating farmers according to their attitude towards risk, it is possible to transform those risk takers into commercial orientation by supporting them to adopt advanced technologies. Capacity building training is one such enabler. Dilla cluster showed the lowest potential for the production of current maize cultivars thus rendering small-scale farmers, who merely rely on rain for maize production, vulnerable to climate risks. The low productivity could be due to unsuitability of the microclimate or broken adaptability of cultivars as stated by Zhang et al. (2021), and implies the need for renewal of hybrids and maize cultivars with merits of shade tolerance and adaptability for cropping mixtures suitable for the environment. Adoption of rigorous adaptation options including the use of seasonal forecasts during growing seasons would also aid through near real time agro-climate advisory services extension to the target users. Thus, the Dilla and Bilate CDFs lie entirely to the left of Shamana and Hawassa for all the higher risk levels, implying how Dilla and Bilate clusters have a high probability of failure in maize production, compared to the Shamana and Hawassa clusters, and that at each point of maize yield, the later scenarios have less risk (Fig. 3A–F). This result signifies that the Dilla and Bilate clusters deserve strategies that foster climate risk adaptation responses under the current climatic conditions.

Simulation of maize yield across baseline, early, mid- and late century

The median yield of BH-540 was 4.0, 5.9, 4.8, 4.3, 5.8, 3.9 and 1.5 t ha^{-1} during baseline, early, mid- and late century under RCP4.5 and early, mid-and late century during RCP8.5 GHGs emission scenario, respectively (Fig. 4A). Similarly, 4.3, 5.7, 4.8, 4.0, 5.3, 2.8 and 1.5t ha^{-1} is obtained from cultivar BH-546 during baseline, early, mid- and late century under RCP4.5 and early, mid-and late century during RCP8.5, respectively (Fig. 4B). The median yield of BH-547 was 4.5, 5.6, 4.3, 4.1, 5.8, 3.9 and 1.7t ha^{-1} during baseline, early, mid- and late century under RCP4.5 and early, mid-and late century during RCP8.5, respectively (Fig. 4C).

Moreover, 4.4, 4.9, 4.1, 4.0, 5.5, 3.5 and 1.6t ha^{-1} of median yield is obtained from cultivar *Shala* during baseline, early, mid- and late century under RCP4.5 and early, mid-and late century during RCP8.5, respectively (Fig. 4D). The median yield of *Shone* was 4.5, 5.7, 4.2, 3.7, 5.8, 3.3 and 1.3t ha^{-1} during baseline, early, mid- and late century under RCP4.5 and early, mid-and late century during RCP8.5 GHGs emission scenario, respectively (Fig. 4E). The best performance of cultivars *Shone, Shala, BH-546* and BH-547 was obtained in the early-century across RCP 8.5 than RCP 4.5 with maize yields over 6t ha^{-1} in some locations (Fig. 4). Thus, the yield change ranged from −22% (*Shone*) to + 22.7 (BH-546) in Shamana, 1.4% (BH-546) to + 18.1 (BH-540) in Bilate, −17.3% (*Shone*) to + 31 (BH-540) in Hawassa, −11.5% (*Shala*) to 20.2 (BH-540) in Dilla under medium emission scenarios during 1950s compared to baseline (Fig. 5). Under high emission scenarios, yield deviations ranged from −18.4 (BH-540) to −37% (*Shone*) in Shamana, from −3.6 (*Shone*) to −26% (BH-546) in Bilate, −24.7 (BH-546) to −49.2% (*Shone*) in Hawassa, from −14.7 (*Shone*) to −29.7% (BH-546) compared to baseline in Dilla during 1950s (Fig. 5). Under high emission scenario during 1970s, the performance of cultivar BH-540 was lower by 55.6, 62.5, 58.5 and 70% in Shamana, Bilate, Dilla and Hawassa clusters, respectively compared to baseline. For BH-546, the yield loss was 56.6, 68.9, 63 and 68.1%, in that order. The yield performance was reduced by 63.9, 57, 64.8, 63.5% in BH-547; 63.4, 54.5, 59.9, 63.5 in *Shala* and 72.4, 52.6, 76.7 and 65.5% in *Shone* in that respective order compared to baseline.

Discussion

Genetic coefficients

The genetic coefficient differences in Table 3 can be explained by variations in the rate of development and accumulation of dry matter, as well as by differences in the characteristics of vernalization, photoperiod response, duration of grain filling, phyllochron interval, and number of grains per ear of each variety (Iglesias 2006; Adnan et al 2017). The greatest thermal time delay between successive leaf tips, for example, was shown by the highest PHINT values (74.91 °C) for *Shone*, indicating a slow rate of leaf emergence. In the end, this establishes the capacity to correct growth and yield variables while developing vegetative infrastructure. The range of the DSSAT cultivar database was met by the chosen and created cultivar-specific characteristics. Therefore, we may use model produced genetic coefficient for further studies.

Evaluation of DSSAT 4.8 model

A small yield range and a few days of inaccuracy are indicated by the majority of the simulated and observed data, which is near to a 1:1 line (Fig. 2a and b). Other researchers have also reported that the DSSAT model underestimated grain yield and harvest index while overestimating kernel mass, grain N, and total N uptake. They have attributed this to a very warm period during grain filling (Vucetic 2011; Araya et al. 2015; Abedinpour and Sarangi 2018). This could be because water extraction under the simulation was done earlier than in field experiments with water deficit conditions (López-Cedrón et al. 2008). As a matter of fact, the model has underestimated days to maturity in BH-547 and Shone and overestimated them in BH-540, BH-546, and Shala. According to previous research work, which showed a difference of up to 0.20% between simulated and observed with better modeling, the underestimating of simulated grain yield in this experiment by 0.095% could be regarded as a good assessment (Alexandrov et al. 2001). Using the DSSAT CERES-maize model, Feleke et al. (2021) obtained a similar model overestimation result for late-maturing cultivars at Ambo. The relative mean square error (RMSE) and normalized root mean square percentages for grain yield, anthesis dates, and maturity dates correlate to good to adequate ratings, and the results were within allowable bounds; these findings are consistent with those of Mohammed et al. (2022),

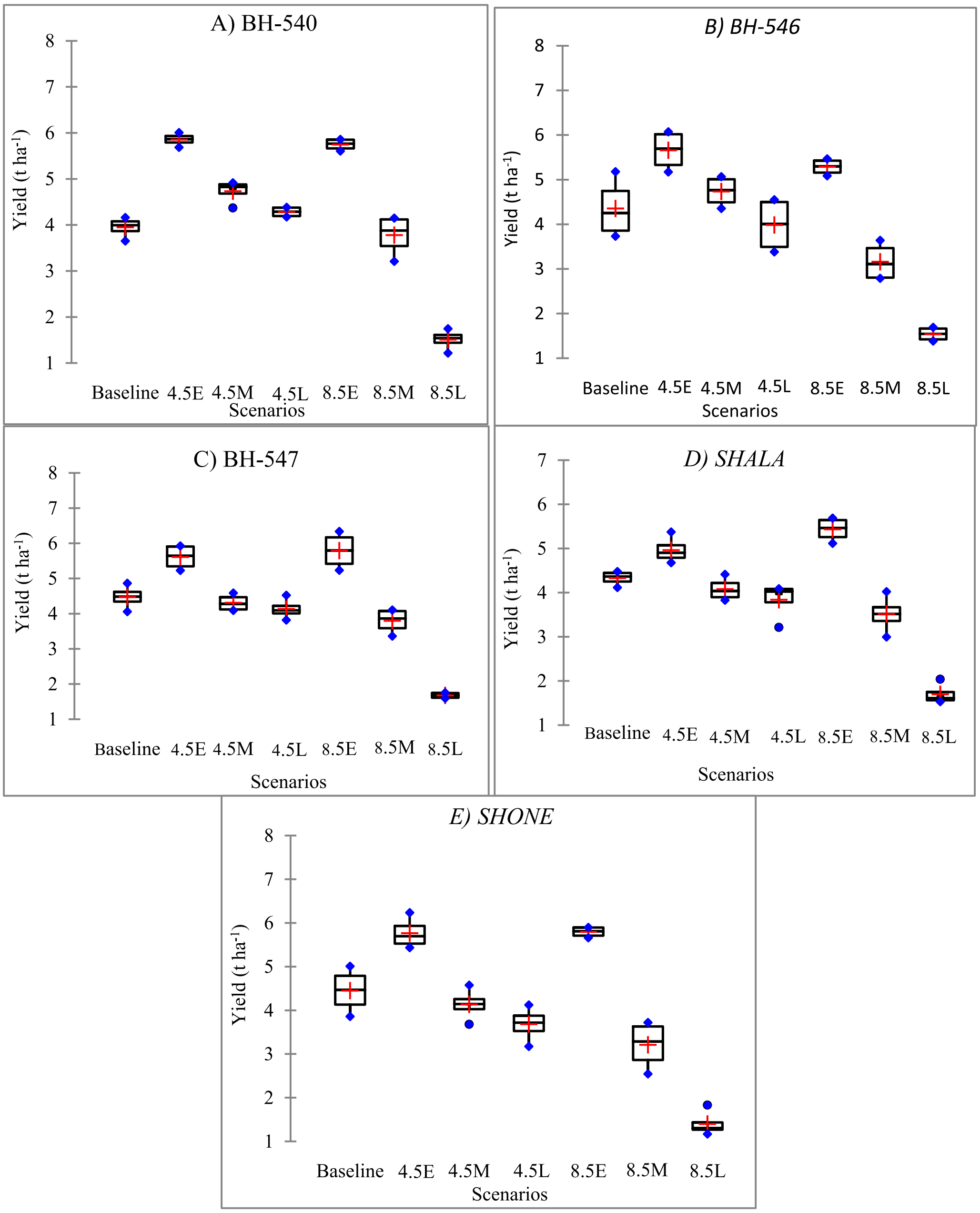

Fig. 4 Maize yield (t ha^{-1}) across RCP 4.5 and 8.5 during baseline, early, mid- and late century (RCP 4.5 and 8.5 stand for medium and high GHGs emission scenarios, E, M and L stand for early, medium and late century, respectively)

Feleke et al. (2021), Kassie et al. (2014), and Liben et al. (2018). The grain yield parameter had the lower error rate, days to maturity had an intermediate percentage, and days to anthesis had the bigger percentage. As indicated by the negative error percentages, the model slightly underestimated the grain yield for the *Shala*, BH-540, BH-546, and BH-547 varieties, while slightly overestimated the grain yield for the Shone variety (Table 4). For the majority of data, the d statistic, or index of agreement, was closer to 1. When the temperature difference between the daily maximal and minimal temperatures remain as small as possible, the DSSAT model appears to predict a higher rate of grain filling (Wilkens & Singh 2001).

Environmental effect on cultivars

A cultivar of *Shala* yielded 7.6 t ha^{-1} in the Shamana cluster, which is considerably ($P<0.05$) greater than the yields of cultivars BH-540, BH-546, and BH-547. Cultivar

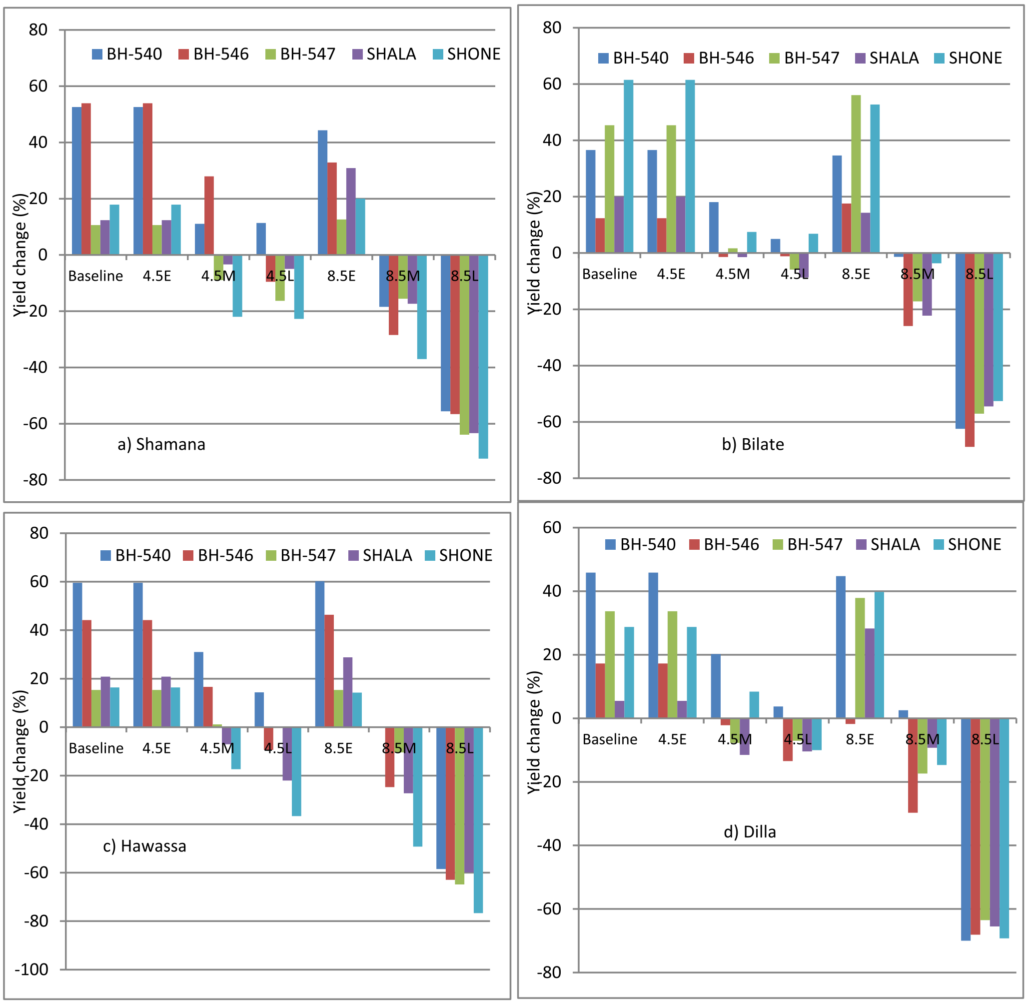

Fig. 5 Yield change (%) of maize cultivars across RCP 4.5 and 8.5 during baseline, early, mid- and late century at Shamana, Bilate, Hawassa and Dilla clusters

Shone outperformed other cultivars in the Bilate cluster, yielding a much greater yield (5.4 t ha^{-1}). Cultivar *Shone* outperformed the other cultivars (9.2 t ha^{-1}) in the Hawassa cluster. The Shamana cluster's lowest yield was recorded because of BH-546 (7.1 t ha^{-1}). Cultivar *Shone* outperformed the other cultivars evaluated in this trial, yielding 5.9 t ha^{-1} in the Dilla cluster. *Shala* and *Shone* were higher yielding cultivars that provided greater yields across varied environments. Thus, in order to increase performance from other cultivars, it is necessary to invest more in correcting susceptible traits of the cultivars. The Dilla cluster's lowest yield (3.6 t ha^{-1}) was attributed to BH-540. Throughout the 1990–2020 era, cultivar *Shone* exhibited substantially ($P<0.05$) longer days to anthesis across all clusters, whereas cultivar BH-547 showed significantly ($P<0.05$) shorter days to anthesis across all clusters. Compared to the other cultivars, *Shone* or *Shala* may have a longer growth period and a faster growth rate, which might account for their higher grain production. In any event, the environment in Hawassa is ideal for these medium-maturing hybrids (Fig. 3), which may be because of the cluster's rainfall and the rising trend in technology usage. The Dilla cluster has the lowest potential for producing maize, which may be related to the region's declining rainfall pattern (0.421 mm year^{-1} (Markos et al. 2023a). In Bilate, Shamana, and Dilla, cultivars BH-540, 546, and 547 seldom ever yield more than 4 t ha^{-1}. The current conclusion is consistent with Sharada et al. (2020) and Rising and Devineni's (2020) recommendation that, in light of climate change, shifting crops, cultivars and locations used for maize production are essential measures. Some writers also suggested using breeding to adjust to climate change in order to correct related traits, which really calls for several selection cycles in maize breeding (Raisnanen and Raty 2003; Zhang et al. 2021).

Performance of cultivars in the current and future climate

In historic climate conditions, *Shone* outperforms the other cultivars across production clusters consistently (Fig. 4). Other cultivars performed differently in different clusters. While cultivar BH-540 was the most adaptable to climate change in the 2050s, cultivar *Shone* was the least; other cultivars shown intermediate tolerance, even in scenarios with medium emissions. Cultivars cultivated in Ethiopia's southern central rift valley will thus see a decline in yield in the 2050s (Fig. 5). This is true even though sub-Saharan Africa is expected to have a 60% rise in food demand, placing the southern Central Rift Valley at the most danger to food security (Alexandratos and Bruinsma 2012). If adaptation measures are not implemented, maize yields in the 2070s might drop to between 54.7 (cultivar *Shala* cultivated at Bilate) to 76.7% (cultivar *Shone* grown at Hawassa).

The present figure exceeds that of Rising and Devineni (2020), who predicted a 37% decline in corn yields in the states' in 2070s under RCP 8.5. This is also in line with the conclusions of the IPCC (2018) evaluations, which confirmed the anticipated decrease in the productivity of vital cereals in Southeast Asia, Central and South America, sub-Saharan Africa. A variety of physiological, biochemical, and molecular processes resulting from an increase in extreme weather events, changes in pest and disease patterns, increases in minimum and maximum temperature, and variability in precipitation amount relative to early century period (2011–2039) could be the cause of the yield decline, which would ultimately reduce maize yield (Markos et al. 2023b; Zhang et al. 2021; IPCC 2018). When compared to other hybrids, the output of high-yielding cultivars like *Shone* drastically declines, necessitating the need to increase adaption choices like as heat stress tolerance, drought tolerance, and resistance to newly developing pests and diseases. However, given that yields were significantly lower than 2 t ha^{-1} in the RCP 8.5, none of the cultivars now in use could withstand the impacts of rising temperatures and erratic rainfall. The potential impacts of these findings on future agricultural policies and practices highlights the need for improved germplasm suited for high-temperature and water-limited settings (Van Ettana et al. 2019). It might have been possible to decrease the sub-optimal performance of cultivars during past and future weather conditions by promptly disseminating high-quality weather advisory information and agricultural inputs (Mamo et al. 2013). However, countries are looking for zero hunger in their Sustainable Development Goals (https://sdgs.un.org/goals) to address food security issues. If these are to be realized, there should be a determined and ongoing effort to maintain and improve parental lines, reduce greenhouse gas emissions, and address the potential causes of yield decline, which includes loss of hybrid vigor, breakage of adaptability, or deterioration of inbred lines of these three-way crosses during the late century. The potential benefits of implementing the suggested adaptation strategies is promising but the challenges of generating and adopting the adaptation strategies calls for prioritization by policy makers and investment in the sector in line with climate change adaptations.

Conclusion and recommendations

Studying how, maize, the second most extensively cultivated crop and its cultivars respond to various production conditions under the current and projected climate is so essential under conditions of Southern Central Rift Valley of Ethiopia. Using field experimental data, the DSSAT version 4.8 was calibrated and validated for the environment. The normalized root mean square percentage, d-statistics and root mean squares of error for anthesis dates, maturity dates and grain yield during calibration and validation can be classified as good to excellent ratings. These figures confirm that the DSSAT 4.8 modeling has been used effectively for the development and production of hybrid maize. The outcomes of the 1:1 lines further demonstrated that, under the statistical significance level, the simulated findings and actual values agreed closely. In light of this, DSSAT version 4.8 may be advantageous for digitizing agro-weather advisory services and distributing them to the intended customers in the study clusters. The simulation experiment recommended the *Shala* variety (7.6 t ha^{-1}) for the Shamana cluster and the *Shone* variety for Bilate (5.4 t ha^{-1}), Hawassa (9.2 t ha^{-1}), and Dilla (5.9 t ha^{-1}) clusters. Nonetheless, yields in the Shamana, Bilate, Hawassa, and Dilla clusters vary from 2.2 to 7.6, 3.7 to 5.4, 7.1 to 9.2, and 3.3 to 5.9 t ha^{-1} in that order. Observations across the time period and emission scenarios revealed that cultivars *Shala* and BH-540 fared better against climatic change than cultivars BH-546, BH-547, and *Shone* throughout the early century. No investigated cultivar demonstrated tolerance to climate change throughout medium and high emission scenarios during the mid and late century, indicating the need for imperative decrease in greenhouse gas emissions and widespread adoption of creative adaptation solutions, which actually calls for development of policies and guidelines that assure the cases in point. It was also inferred that farmers who take more risks can aim to produce higher yields from any cultivar in any of the locations, but they must use cutting-edge technologies and techniques to overcome the challenges involved in achieving their desired yields. Risk-averse farmers can seek lower yields in any of the clusters from any of the cultivars. Compared to the Shamana and Hawassa clusters, the Dilla and Bilate clusters have a higher chance of risk in maize production, highlighting the priority needed for measures that improve responses to climate change and adaptation. A risk-taking farmer can aim for greater yields in any of the areas, but to do so, they must invest in better technologies and techniques that will help them decrease the degree of risk they are targeting. Because lower rainfall areas will experience declining maize yields, appropriate adaptation strategies are needed to mitigate the danger of climate change. In addition, it is imperative that researchers, other scholars, and decision-makers move quickly to commence breeding initiatives for maize crop that target climate change adaptation and associated insect pest/disease resistance/tolerance in order to efficiently manage potential climate risks in the middle and late century periods. It can be deduced that the DSSAT version 4.8 could be effectively used to simulate the phenology, growth, and yield of hybrid maize plants grown in the southern central Ethiopian rift valley. It could also be used to assess the impact of climate change and develop adaptation plans for both the current and future climate.

Abbreviations

CCLM4	COSMO Model in Climate Mode, version 4
CERES	Crop Environment Resource Synthesis
CHEM	Weather-chemistry prediction model
CNRM-CM5	CNRM-GAME Météo-France/CNRS) and CERFACS Earth System Model
CNRM-CM5.1	Centre National de Recherches Météorologiques Coupled Global Climate Model, v 5.1
CORDEX	Coordinated Regional Climate Downscaling Experiment
DSSAT	Decision Support System for Agro- Technological Transfer
EC-EARTH	European Consortium Earth System Model
ESM2M	Earth System Model with Modular Ocean Model version 4 (MOM4) component
GCM	Global circulation model
GFDL	Geophysical Fluid Dynamics Laboratory
HIRHAM (version 5)	Combination of High-Resolution Limited-Area Model (HIRLAM) and the German "ECHAM" Model]
ICHEC	The Irish Centre for High End Computing
MIROC5	Model for Interdisciplinary Research on Climate of the Center for Climate System Research, The University of Tokyo, Japan
MPI-CSC	Max Planck Institute–Climate Service Centre
MPI-ESMLR	Max Planck Institute–Earth System Model, low resolution
NORESM1-M	The Norwegian Earth System Model, version 1 (intermediate resolution)
RACMO22T	Regional Atmospheric Climate Model
RCA	The Rossby Center Atmospheric Model
RCM	Regional climate model
RCP 4.5	Representative concentration pathway
RCP 8.5	Representative concentration pathway
RegCM4	Regional Climate Model version 4.0
REMO	The atmospheric Regional-Scale Model
SOMD-ESD	Empirical: statistical downscaling of NASA's Space Operations Mission Directorate
4.5E, 4.5M and 4.5L	Medium greenhouse gas emission scenario during early, medium and late century, respectively
8.5 E, 8.5M and 8.5L	High greenhouse gas emission scenario during early, medium and late century, respectively

Acknowledgements
The authors acknowledge Hawassa University College of Agriculture School of Plant and Horticultural Sciences for hosting PhD program in Agronomy and the National Meteorology and Climate Change Institute (the then National Meteorology Agency) Hawassa Branch Office for provision of geo-referenced weather data and SARI (Southern Agriculture Research Institute) for sponsoring the study.

Author contributions
D.M.; W.W.—conceptualization; D.M –Data collection; D.M.; G.M.—formal analysis; D.M., G.M.—methodology; D.M.—resources; D.M., G.M.—writing: original draft; and W.W.—writing: review and editing. All authors read and approved the final manuscript.

Funding
All the funding sources are dully acknowledged.

Data availability
The data used in this study will be available from corresponding author upon reasonable request.

Declarations

Ethics approval and consent to participate
The authors declare that they have no known competing financial interests or personal relationships that could have appeared to influence the work reported in this paper.

Consent for publication
The authors agree on the publication of the manuscript.

Competing interests
The authors declare there is no competing interest.

Received: 19 August 2023 Accepted: 13 March 2024
Published online: 21 March 2024

References

Abedinpour M, Sarangi A. Evaluation of DSSAT- Ceres model for maize under different water and nitrogen levels. Pertanika J Sci Technol. 2018;26(4):1605–18.

Abera K, Crespo O, Seid J, Mequanent F. Simulating the impact of climate change on maize production in Ethiopia, East Africa. Environ Syst Res. 2018;7(4):1–12.

Adnan AA, Jibrin MJ, Kamara AY, Abdulrahman BL, Shuaibu AS, Garba LL. CERES-Maize model for determining the optimum planting dates of early maturing maize cultivars in northern Nigeria. Front Plant Sci. 2017;8:1–18.

Aggarwal PK, Banerjee B, Daryaei MG, Bhatia A, Bala A, Rani S, Chander S, Pathak H, Kalra N. Infocrop: A dynamic simulation model for the assessment of crop yields, losses due to pests and environmental impact of agro-ecosystems in tropical environments. II. Performance of the model. Agric Sys. 2006;89:47–67.

Alexandratos N, Bruinsma J. World Agriculture towards 2030/2050: The 2012 Revision. Rome: Food Agriculture Organization of the United Nations; 2012.

Alexandrov V, Eitzinger J, Oberforster M. Adaptation of crop-weather models in Austria and Bulgaria. In Proceedings of the 5th European Conference on Applications of Meteorology. Budapest, Hungary: European Meteorological Society. CD-ROM; 2001.

Araya A, Hoogenboom G, Luedeling E, Hadgu KM, Kisekka I, Martorano LG. Assessment of maize growth and yield using crop models under present and future climate in Southwestern Ethiopia. Agric Meteorol. 2015;214(205):252–65.

Ayalew A, Beyene S, Walley F. Characterization and classification of soils of selected areas in Southern Ethiopia. J Environ Earth Sci. 2015;5(11):116–31.
Bayable G, Amare G, Alemu G, Gashaw T. Spatiotemporal variability and trends of rainfall and its association with Pacific Ocean Sea surface temperature in West Harerge Zone, Eastern Ethiopia. Environ Sys Res. 2021;10(7):1–21.
Bejigo G. Growth and yield response of maize (*Zea mays* L) cultivars with varying rates of nitrogen supply in Halaba District South Ethiopia. Amer J Agric Forest. 2018;6(6):237–45.
Belay A, Demissie T, Recha JW, Oludhe C, Osano PM, Olaka LA, Solomon D, Berhane Z. Analysis of climate variability and trends in Southern Ethiopia. Clim. 2021;9(96):1–17.
Boote K. The DSSAT crop modeling ecosystem. In: Advances in crop modeling for a sustainable agriculture. 2017: 1–45.
Boote KJ, Jones JW, Hoogenboom G, White JW. The role of crop systems simulation in agriculture and environment. Int J Agric Environ Info Sys. 2010;1:41–54.
Chambers JM, Freeny AE, Heiberg RM. Analysis of variance; designed experiments. Statistical models in S. Routledge; 2017, 145–193.
Clarke L, Edmonds J, Jacoby H, Pitcher H, Reilly J, Richels R. Scenarios of Greenhouse Gas Emissions and Atmospheric Concentrations, Sub-report 2.1 A of Synthesis and Assessment Product 2.1 by the US Climate Change Science Program and the Subcommittee on Global Change Research. Department of Energy, Office of Biological & Environmental Research, Washington, 7 DC, USA, 2007, 154.
Demiss M, Beyene S. Characterization and classification of soils along the toposequence of Kindo Koye watershed in Southern Ethiopia. East Afr J Sci. 2010;4(2):65–77.
Derbew S, Dawuro D. Participatory evaluation of maize cultivars under conservation agriculture and conventional practice for moisture deficit areas of Southern Ethiopia. Int J Pure Agric Adv. 2017;1(1):30–7.
Dinku T, Funk C, Peterson P, Maidment R, Tadesse T, Gadain H, Ceccato P. Validation of the CHIRPS satellite rainfall estimates over eastern Africa. Q J R Meteorol Soc. 2018;144(Suppl. 1):292–312.
Feleke HG, Savage MJ, Tesfaye K. Calibration and validation of APSIM–Maize, DSSAT CERES–Maize and AquaCrop models for Ethiopian tropical environments. S Afr J Plant Soil. 2021;38(1):36–51.
Giorgi F, Jones C, Asrar G. Addressing climate information needs at the regional level: the CORDEX framework. Organization (WMO) Bulletin. Geneva: World Meteorological Organization (WMO), 2009, 175–183.
Gobo AE, Abam TKS. Return period analysis as a tool for urban flood prediction in the Niger delta: a case study of Port Harcourt City, Nigeria. J Environ Hydrol. 2006;14:1–12.
Hai-long L, Hong-bin L, Qiu-liang L, Li-mei Z, Hong-yuan W, Ji-zong Z, Ye-ping Z, Sheng-ping L, Shi-juan L, Jing-suo Z, Xiao-xia L. Using the DSSAT model to simulate wheat yield and soil organic carbon under a wheat-maize cropping system in the North China Plain. J Integr Agric. 2017;16(10):2300–7.
Hidoto L. Growth and grain yield response of maize cultivars to conservation tillage in Southern Ethiopia. World J Innov Res. 2021;11(3):52–6.
Hidoto L, Markos D. Towards sustainable maize legume cropping systems: conservation agriculture based intensification, workshop proceeding of conservation based intensification held from 22 to 24 July, Shashamane, Ethiopia; 2019.
Holzworth DP, Snow V, Janssen S, Athanasiadis IN, Donatelli M, Hoogenboom G, White JW, Thorburn P. Agricultural production systems modeling and software: current status and future prospects. Environ Model Softw. 2015;72(1):276–86.
Hoogenboom G, Jones JW, Wilkens PW, Porter CH, Boote KJ, Hunt LA. Decision Support System for Agrotechnology Transfer (DSSAT). Version 4.8, University of Hawaii, Honolulu, USA; 2010.
Iglesias A. Calibration and validation of CERES-wheat and CERES maize in Spain, Universidad Politecnica de Madrid, Hands-on training workshop on V&A assessment, Jakarta, 20–24 March 2006; 2006.
IPCC. Summary for Policymakers. In: Masson-Delmotte V, Zhai P, Pörtner H-O, Roberts D, Skea J, Shukla PR, Pirani A, Moufouma-Okia W, Péan, R Pidcock C, Connors S, Matthews JBR, Chen Y, Zhou X, Gomis MI, Lonnoy E, Maycock T, Tignor M, Waterfield T (Eds.) Global Warming of 1.5 ˚C. An IPCC Special Report on the Impacts of Global Warming of 1.5 ˚C above Pre-Industrial Levels and Related Global Greenhouse Gas Emission Pathways, in the Context of Strengthening the Global Response to the Threat of Climate Change, Sustainable Development, and Efforts to Eradicate Poverty (32 p.). Geneva: World Meteorological Organization; 2018.
Jemal SH. Risks and opportunities from more productive and resilient cropping system strategies in the Central and Southern Rift Valley of Ethiopia, A thesis submitted for the degree of Doctor of Philosophy at The University of Queensland ,Queensland Alliance for Agriculture and Food Innovation (QAAFI), Australia; 2018.
Jones PG, Thornton PK. The Potential impacts of climate change on maize production in Africa and Latin America in 2055. Glob Environ Chang. 2003;13:51–9.
Jones JW, Hoogenboom G, Porter CH, Boote KJ, Batchelor WD, Hunt LA. The DSSAT cropping system model. Eur J Agron. 2003;18:235–65.
Kalra N, Chakraborty D, Sharma A, Rai HK, Jolly M, Chander S, Ramesh KP, Bhadraray S, Barman D, Lal M, Sehgal M. Effect of increasing temperature on yield of some winter crops in North-West India. Curr Sci. 2008;94:82–8.
Kassie BT, Van Ittersum MK, Hengsdijk H, Asseng S, Wolf J, Rötter RP. Climate-induced yield variability and yield gaps of maize (*Zea mays* L.) in the Central Rift Valley of Ethiopia. Field Crop Res. 2014;160:41–53.
Lamsal A, Welch SM, White JW, Thorp KR, Bello NM. Estimating parametric phenotypes that determine anthesis date in *Zea mays*: challenges in combining ecophysiological models with genetics. PLoS ONE. 2018;13(4): e0195841.
Leng G, Hall JW. Predicting spatial and temporal variability in crop yields: an inter-comparison of machine learning, regression and process-based models. Environ Res Let. 2020;15: 044027.
Li K, Guo L, Pan J, Li M. Evaluation of future maize yield changes and adaptation strategies in China. Sustainability. 2022;14:9246.
Liben FM, Wortmann CS, Yang H, Lindquist J, Tadesse T, Gissa DW. Crop model and weather data generation evaluation for conservation agriculture in Ethiopia. Field Crops Res. 2018;228:122–34.
Loha G, Hidoto L. Performance evaluation of maize (*Zea mays* L.) cultivars in low moisture stress area of Southern Ethiopia. Sumerianz J Agric Vet. 2018;1(1):24–9.
López-Cedrón FX, Boote KJ, Piñeiro J, Sau F. Improving the CERES-Maize model ability to simulate water deficit impact on maize production and yield components. Agron J. 2008;100:296–307.
Luhunga PM, Kijazi AL, Changa L, Kondowe A, Ngongolo H, Mtongori H, Kondowe A. Climate change projections for Tanzania Based on highresolution regional climate models from the CORDEX - Africa. Front Environ Sci. 2018;6:1–20.
Ma L, Hoogenboom G, Ahuja LR, Ascough IC, Saseendran SA. Evaluation of the RZWQM-CERES-maize hybrid model for maize production. Agric Syst. 2006;87:274–95.
Mamo G, Getnet M, Legesse G, Mitku T. Integration of information on climate, soil and cultivar to increase water productivity of maize in semi-arid eco-regions of Ethiopia. Ethiop J Agric Sci. 2013;24:123–39.
Markos D, Mamo G, Worku W. Principal component and cluster analyses based characterization of maize fields in southern central Rift Valley of Ethiopia. Open Agr. 2022;7(1):504–19.
Markos D, Worku W, Mamo G. Spatio-temporal variability and rainfall trend affects seasonal calendar of maize production in southern central Rift Valley of Ethiopia. PLOS Clim. 2023a;2(6): e0000218.
Markos D, Worku W, Mamo G. Exploring adaptation responses of maize to climate change scenarios in southern central Rift Valley of Ethiopia. Sci Rep. 2023b;13:12949.
Mekasha GM, Seyoum SA, Lemma AZ. Participatory maize hybrid evaluation for different cropping systems in the central rift valley in Ethiopia. J Plant Breed Crop Sci. 2020;12(4):269–74.
Mohammed A, Yimer E, Gessese B, Feleke E. Predicting Maize (*Zea mays*) productivity under projected climate change with management options in Amhara region, Ethiopia. Environ Sustain Indic. 2022;15: 100185.
Moss RH, Edmonds JA, Hibbard KA, Manning MR, Rose SK, van Vuuren DP. The next generation of scenarios for climate change research and assessment. Nature. 2010;463:747–56.
Mulungu DMM, Mukama E. Evaluation and modelling of accuracy of satellite-based CHIRPS rainfall data in Ruvu subbasin, Tanzania. Model Earth Syst Environ. 2023;9:1287–300.
Niang I, Ruppel OC, Abdrabo MA, Essel A, Lennard C, Padgham J, Urquhart P. 2014. Africa. In: Climate Change 2014 Cambridge University Press, Cambridge, United Kingdom, and New York, NY, USA, pp. 1199–1265.

Ojara MA, Yunsheng L, Ongoma V, Mumo L, Akodi D, Ayugi B, Ogwang BA. Projected changes in East African climate and its impacts on climatic suitability of maize production areas by the mid-twenty-first century. Environ Monit Assess. 2021;193:831.
Ongoma V, Chen H, Gao C. Projected changes in mean rainfall and temperature over East Africa based on CMIP5 models. Intern J Climatol. 2018;38:1375–92.
Pereira L. Climate change impacts on agriculture across Africa. Oxford Res Encycl Environ Sci. 2017. https://doi.org/10.1093/acrefore/9780199389414.013.292.
Raisanen J, Raty O. Projections of daily mean temperature variability in the future: cross-validation tests with ENSEMBLES regional climate simulations. Clim Dyn. 2003;41:1553–68.
Rani SU, Kiran LP, Naik BS, Rani NV, Mahendra SB. Application of non-parametric statistical tools in analysing the climate data through XLSTAT. Contemp Perspect Sci Technol Res. 2023;1(8):1–12.
Riahi SR, Paul R, Ron S, van Detlef V, John W, Tom W, Jean PY, Monika Z. Towards new scenarios for analysis of emissions, climate change, impacts, and response strategies. Geneva: Intergovernmental Panel on Climate Change; 2008. p. 132.
Rising J, Devineni N. Crop switching reduces agricultural losses from climate change in the United States by half under RCP 8.5. Nat Commun. 2020;11:4991.
Ritchie JT, Nesmith DS. Temperature and crop development. In: Hanks J, Ritchie JT, editors. Modeling plant and soil systems. Madison: ASA-CSSA-SSSA; 1991. p. 6–27.
Sharda V, Mekonnen MM, Ray C, Gowda PH. Use of multiple environment variety trials data to simulate maize yields in the Ogallala Aquifer Region: a two model approach. J Am Water Resourc Assoc. 2020;57:1–15.
Shengu MK, Tilahun B. Heritability and performance of single cross maize hybrids in dilla and abaya areas. Int J Res Sci Innov. 2018;3(7):1–5.
Shivakumar A, Taliotis C, Howells M. The impact of climate change on crop production in water and energy implications. An integrated systems assessment with water and energy implications. Water. 2019;11:1805.
Sorsa Z, Mesfin K. Evaluation of yield performance and variation on its adaptation-related traits of quality protein maize (qpm) (*Zea mays* L.) cultivars at selected woredas of Wolaita Zone, Ethiopia. Int J Plant Breed Genet. 2015;9(4):255–61.
Tofa AI, Kamara AY, Babaji BA, Akinseye FM, Bebeley JF. Assessing the use of a drought-tolerant variety as adaptation strategy for maize production under climate change in the savannas of Nigeria. Sci Rep. 2021;11:8983.
van Ettena J, de Sousa K, Aguilarc A, Barriosc M, Cotoa A, Dell'Acquad M, Faddae C, Gebrehawaryate Y, van de Gevel J, Gupta A, Kirosh AY, Madriza B, Mathurg P, Mengistu DK, Mercado L, Mohammed JN, Paliwal A, Pe ME, Quiros CF, Rosas JC, Sharma N, Singhk SS, Solanki IS, Steinke J. Crop variety management for climate adaptation supported by citizen science. PNAS. 2019;116(10):4194–9.
Vucetic V. Climate change and agriculture paper modeling of maize production in croatia: present and future climate. J Agric Sci. 2011;149:145–57.
Wang X, Miao Y, Batchelor WD, Dong R, Kusnierek K. Evaluating model-based strategies for in-season nitrogen management of maize using weather data fusion. Agric Forest Meteorol. 2021;108564:308–9.
Wendimeneh D. Characterization and classification of the soils of upper sala watershed in Dilla zuria district of Gedeo Zone, Southern Ethiopia, Msc Thesis in Soil Science, Haramaya University, Ethiopia; 2010.
Whisler FD, Acock B, Baker DN, Fye RE, Hodges HF, Lambert JR, Lemmon HE, McKinion JM, Reddy VR. Crop models in agronomic systems. Adv Agron. 1986;40:141–208.
White JW, Hoogenboom G, Kimball BA, Wall GW. Methodologies for simulating impacts of climate change on crop production. Field Crops Res. 2011;124:357–68.
Wilkens P, Singh U. A code-level analysis for temperature effect in the CERES models, In Modeling temperature response in wheat and maize, Proceedings of a Workshop (Ed. J. W. White), 2001, pp. 1–7. El Batán, Mexico: CIMMYT.
Willems P, Vrac M. Statistical precipitation downscaling for small-scale hydrological impact investigations of climate change. J Hydrol. 2011;402:193–205.
Willmott CJ. Some comments on the evaluation of model performance. Bull Am Meteor Soc. 1982;63:1309–13.
Yang JM, Yang JY, Liu S, Hoogenboom G. An evaluation of the statistical methods for testing the performance of a crop simulation model with observed data. Agric Syst. 2014;127(1):81–9.
Yimer SM, Bouanani A, Kumar N, Tischbein B, Borgemeister C. Assessment of climate models performance and associated uncertainties in rainfall projection from CORDEX over the Eastern Nile Basin, Ethiopia. Climate. 2022;10:95.
Zhang L, Zhang Z, Tao F, Luo Y, Cao J, Li Z, Xie R, Li S. Planning maize hybrids adaptation to future climate change by integrating crop modelling with machine learning. Environ Res Lett. 2021;16: 124043.

Publisher's Note